# Timescales of lateral sediment transport in the Panama Basin as revealed by radiocarbon ages of alkenones, total organic carbon and foraminifera

Stephanie KUSCH[1,2]*, Timothy I. EGLINTON[3], Alan C. MIX[4], Gesine MOLLENHAUER[1,2]

1 Alfred-Wegener-Institut für Polar- und Meeresforschung, Am Handelshafen 12, 27570 Bremerhaven, Germany
(Stephanie.Kusch@awi.de)
(Gesine.Mollenhauer@awi.de)

2 Fachbereich Geowissenschaften, Universität Bremen, Klagenfurter Str., 28359 Bremen, Germany

3 Department of Marine Chemistry and Geochemistry, Woods Hole Oceanographic Institution, Woods Hole, Massachusetts 02543, USA
(teglinton@whoi.edu)

4 College of Ocean and Atmospheric Sciences, Oregon State University, Corvallis, Oregon 97331, USA
(amix@coas.oregonstate.edu)

* corresponding author: phone +49 421 218 65075; fax +49 421 218 65099

**Abstract**

Paired radiocarbon measurements on haptophyte biomarkers (alkenones) and on co-occurring tests of planktic foraminifera (*Neogloboquadrina dutertrei* and *Globogerinoides sacculifer*) from late glacial to Holocene sediments at core locations ME0005-24JC, Y69-71P, and MC16 from the south-western and central Panama Basin indicate no significant addition of pre-aged alkenones by lateral advection. The strong temporal correspondence between alkenones, foraminifera and total organic carbon (TOC) also implies negligible contributions of aged terrigenous material. Considering controversial evidence for sediment redistribution in previous studies of these sites, our data imply that the laterally supplied material cannot stem from remobilization of substantially aged sediments. Transport, if any, requires syn-depositional nepheloid layer transport and redistribution of low-density or fine-grained components within decades of particle formation. Such rapid and local transport minimizes the potential for temporal decoupling of proxies residing in different grain size fractions and thus facilitates comparison of various proxies for paleoceanographic reconstructions in this study area. Anomalously old foraminiferal tests from a glacial depth interval of core Y69-71P may result from episodic spillover of fast bottom currents across the Carnegie Ridge transporting foraminiferal sands towards the north.

**Keywords**

compound-specific radiocarbon dating
alkenones
lateral sediment transport
Panama Basin
Eastern Equatorial Pacific

## 1. Introduction

The Equatorial Pacific plays a major role in the global carbon and nitrogen cycle via oceanic biological productivity and ocean-atmosphere gas exchange (Chavez and Barber, 1987; Pennington et al., 2006). Regionally high primary productivity is maintained by upwelling along the equatorial divergence (Kessler, 2006; Wyrtki, 1967), pumping organic carbon to the deep sea. However, the Equatorial Pacific is presently a net source of $CO_2$ to the atmosphere since its major nutrients are not fully consumed perhaps due to iron limitation (Behrenfeld et al. 1996; Kolber et al. 1994). Understanding the climate history of this region is important for understanding the interaction of physical and biological processes related to climate change.

The Panama Basin has been intensively studied for its climate and paleoproductivity history over glacial-interglacial timescales based on a wide range of proxies (Loubere, 1999; Loubere, 2000; Loubere et al., 2003; Loubere et al., 2004; Loubere and Richaud, 2007; Lyle et al., 2002; Lyle et al., 2005; Lyle et al., 2007; Martinez et al., 2006; Paytan et al., 1996; Pedersen, 1983; Pisias and Mix, 1997; Sarnthein et al., 1988). A conflict has emerged in terms of the past sedimentation dynamics of this region. Accumulation rates of sedimentary constituents related to marine productivity and vertical carbon export (e.g., organic carbon, calcium carbonate or barite) indicate higher glacial export rates compared to interglacials (Lyle et al., 2002; Paytan et al., 1996; Pedersen, 1983; Sarnthein et al., 1988), whereas proxies normalized to a "constant flux" proxy (i.e. $^{230}Thorium_{excess}$) (Loubere, 1999; Loubere, 2000; Loubere et al., 2003; Loubere et al., 2004) and faunal assemblages (Loubere, 1999; Martinez et al., 2006) imply constant or reduced glacial productivity. The latter findings imply lateral particle transport and sediment focusing processes play an important role in this region. Such transport might also account for conflicts among paleoceanographic proxies carried in different grain-size fractions (Mix, 2006).

Moore et al. (1973) demonstrated that the distribution of biogenic sediments (carbonate and opal) in the Panama Basin does not match the pattern which should be derived from the overlying primary productivity, and inferred winnowing and lateral transport of fine-grained material. Using textural analysis Van Andel (1973) estimated that winnowed fine-grained material from the surrounding volcanic ridges contributes at least 40-50% of total sediment accumulation in the Panama Basin. Honjo (1982) showed that the lithogenic fraction in sediment traps at 3560m depth was several times higher than the corresponding fraction from 890 and 2590m depth, implying that a major fraction of the lithogenic particles reaching the deep Panama Basin did not originate from overlying surface waters. A combined photo-optical and sediment trap approach reveals that marine snow abundances cannot account for the particle fluxes collected by traps, requiring resuspension from the sediment water interface and subsequent lateral transport (Asper et al., 1992).

Radiocarbon measurements of seawater dissolved inorganic carbon (DIC), particulate inorganic and organic carbon (PIC and POC) from different water depths as well as sediment fluff inorganic and organic carbon (SIC and SOC) require a source of old carbon in the deep water, which is at least partly derived from resuspended sediment (Druffel et al. 1998).

Using the $^{230}$Thorium normalization method, several authors suggested that the sediment accumulation maxima observed in glacial sediments from the Panama Basin might be an artifact resulting from lateral supply rather than paleoproductivity (Kienast et al., 2007; Loubere et al., 2004; Marcantonio et al., 2001). Kienast et al. (2007) report $^{230}Thorium_{excess}$ ($^{230}Th_{xs}$) derived focusing factors ($\Psi$) for cores from the Panama Basin as high as $\Psi$=7.5, implying substantial contribution of laterally supplied sediment. Nevertheless, the applicability of $^{230}$Th method in the Equatorial Pacific and particularly in the Panama Basin remains a subject of debate (Broecker, 2008; Francois et al., 2007; Kienast et al., 2007; Lyle et al., 2005; Lyle et al., 2007; Siddall et al., 2008).

Comparison of radiocarbon ages of molecular fossils of marine phytoplankton such as the haptophyte-derived alkenones with those of co-occurring calcareous microfossils of planktic foraminifera can independently be used to identify aged allochthonous material supplied via lateral sediment transport processes (Mollenhauer et al., 2003; Ohkouchi et al., 2002). Organic matter is associated with the low-density fraction and is prone to resuspension. Critical shear velocities for resuspension of phytodetritus range from 0.4 to 0.9 cm/s (Beaulieu, 2002; Thomsen and Gust, 2000), considerably less than the critical shear velocities of >1.2 cm/s needed to resuspend foraminifera of ~200-400 µm diameter (assuming the physical properties of sand) (Ziervogel and Bohling, 2003). Thus transport of particles by currents can lead to significant spatial and also temporal offsets between organic matter (alkenones and TOC) and co-occurring foraminifera.

Ohkouchi et al. (2002) reported radiocarbon age offsets of up to 7000 $^{14}$C years between alkenones and planktic foraminifera from identical sediment depth intervals from the Bermuda Rise. They concluded that alkenones were originally deposited at the Canadian Margin where they had been resuspended and transported to the Bermuda Rise. Similar processes were identified by Mollenhauer et al. (2003) for the Benguela upwelling area. Alkenones were found to be approximately 2500 $^{14}$C years older than co-occurring planktic foraminifera, which was interpreted as the result of continuous cycles of resuspension and redeposition of particles originating from the inner shelf off Namibia.

The lateral displacement of sediment constituents associated with different grain-size classes, however, does not necessarily lead to a temporal offset in their radiocarbon contents. Mollenhauer et al. (2006) showed combined $^{14}$C and $^{230}Th_{xs}$ data for the Argentine Basin. In this region, independent evidence exists for lateral displacement of alkenone-bearing particles (Benthien and Müller, 2000; Rühlemann and Butzin, 2006). While $^{230}Th_{xs}$ derived focusing factors indicate lateral transport, radiocarbon ages of

alkenones and foraminifera were similar, implying that lateral advection in the Argentine Basin occurs rapidly after sedimentation, and moves essentially modern material (Mollenhauer et al., 2006).

Here we present radiocarbon data for planktic foraminiferal carbonate, total organic carbon (TOC) and alkenones for three cores in the Panama Basin. The good age agreement between most of these different sediment constituents suggest minimal supply of pre-aged organic material of either marine or terrigenous origin. Considering the multiple lines of evidence for occurrence of lateral sediment transport in the Panama Basin, we conclude that lateral transport of the easily-resuspendable, low-density sediment fraction occurs syn-depositionally.

## 2. Study Area

The Panama Basin is located in the Eastern Equatorial Pacific off the coast of Central America and northwestern Southern America (Figure 1). It is relatively isolated from the (Central) Equatorial Pacific by the volcanic Cocos and Carnegie Ridges on the north and south, respectively, and the Galapagos Platform in the west. Underlying the equatorial divergence upwelling region, high rates of primary productivity result in high biogenic particle export from the surface waters to the seafloor. The productivity in the euphotic zone above the Southern Panama Basin is estimated at ~600mg C/m²/day with a biomass of approximately 0.5 mg Chl/m³ The productivity in the Central Panama Basin is less pronounced at ~300-400mg C/m²/day and ~0.3mg Chl/m³ biomass (Behrenfeld and Falkowski 1997; Moore et al., 1973; Pennington et al., 2006; http://giovanni.gsfc.nasa.gov (2002-2008)).

The Panama Basin area is influenced by bottom currents from the Peru Basin, entering through the Ecuador Trench with a sill depth of 2920m. Water masses disperse north- and westward off northern Ecuador and penetrate into the SW Panama Basin south of the Malpelo Ridge where they spread to the north and the south (Laird, 1971; Lonsdale, 1977). An additional inflow-passage into the Panama Basin exists across the central saddle of the Carnegie Ridge located between 85° and 86°W with a sill depth of 2330m. Here, an outcrop of the acoustic basement indicates erosion (or non-deposition) of sediment which is up to 400m thick on the adjacent ridge flanks (Lonsdale, 1977; Malfait and Van Andel, 1980). Erosional valleys up to 400m deep continue from the saddle incision down the northern flank of the Carnegie Ridge. Temperature profiles within the Panama Basin imply that episodic spillover is more likely than a constant flow across the Carnegie Ridge. The cause and frequency of these spillover events is unknown and reliable hydrographic data is lacking (Lonsdale, 1977).

## 3. Materials and Methods

We used deep-sea sediment cores from three locations in the Panama Basin (Table 1). Core ME0005A-24JC was taken during R/V *Melville* cruise ME0005A in 2000, while the neighboring core Y69-71P was taken in 1969 on board R/V *Yaquina* during cruise YALOC69. Both cores were retrieved just north of the Carnegie Ridge in an area of abyssal hills, which is part of a narrow east-west trending trough (Figure 1). Y69-71P was collected mid-slope, while ME0005A-24JC was taken within an adjacent but separate abyssal valley about 10km south of Y69-71P. Samples of 110-136g wet weight were taken from core intervals spanning approximately 5 cm and represented late glacial to Holocene sediments (Table 2). For both cores $^{230}Th_{xs}$ data are available (Kienast et al. 2007).

Additionally multicorer core MC16 from the Central Panama Basin was chosen in order to reconstruct the age relationships of the different sediment constituents in an area with minor influence of lateral advection (Kienast et al. 2007). Core MC16 was taken during R/V *Knorr* campaign in 2005 (KNR 182-9), sampled in 1 cm slices on board ship and stored at -20°C until further analysis. Core slices of 3 sub-cores were re-combined in order to obtain sufficient material for all analyses.

Samples were freeze-dried and homogenized prior to further treatment. Co-occurring alkenones and planktic foraminifer tests were isolated from each sample and radiocarbon dated. For TOC radiocarbon analyses, subsamples of the freeze-dried samples of 100mg-500mg (equivalent to 1 mg organic carbon) were used.

### 3.1 Alkenone Purification

Alkenones were extracted from 30 to 40g of freeze-dried and homogenized sediments using Soxhlet extraction or Accelerated Solvent Extraction (ASE) and purified following the analytical procedures of Ohkouchi et al. (2005b). Total lipid extracts were saponified with 0.5M solution of KOH in MeOH for 3 h at 85°C. After cooling, up to 90% of the solvent was evaporated under a stream of nitrogen and neutral lipids were extracted into hexane five times. The neutral fraction was further separated into three polarity fractions by use of a silica gel column (1% de-activated $SiO_2$, 0.063-0.2mm mesh size, column: 6mm i.d. x 4cm) eluting hydrocarbons using 4ml hexane, ketones and aldehydes using 4ml hexane:$CH_2Cl_2$ (1:2 v:v), and alcohols using 4ml MeOH.

Urea adduction (Marlowe et al., 1984) was performed on fraction 2 to separate straight-chain ketones/aldehydes from branched constituents. For this purpose, the samples were dissolved in a hexane:$CH_2Cl_2$ (2:1 v:v, 4.5ml) solution and a saturated urea solution (40g/l in MeOH, 1.5ml) was added dropwise. Samples were refrigerated for 15 min followed by removal of solvents under a stream of nitrogen. These steps were repeated twice. Afterwards urea crystals were rinsed with hexane five to seven times to recover non-adducted (branched and cyclic) components. Subsequently, urea crystals

were dissolved in Seralpure water and extracted into hexane five to seven times. The straight-chain fraction was then applied to a column containing $AgNO_3$-coated silica gel to separate saturated ketones (4ml $CH_2Cl_2$) from unsaturated ketones (4ml ethyl acetate or ether). To ensure maximum recovery, a third fraction using 4ml MeOH was eluted. Resulting di-, tri- and tetra-unsaturated ketones were finally cleaned using a silica gel column (1% de-activated $SiO_2$, mesh size 0.063-0.2mm, column 6mm i.d. x 4mm) eluting with 4ml hexane:$CH_2Cl_2$ (1:2 v:v) to remove potential contamination introduced during the analytical procedures.

Following each analytical step, purification of the samples was monitored by analysis of subsamples (representing 0.1% of total sample) using an HP5890 series chromatograph equipped with a flame ionization detector.

### 3.2 Foraminifera

Tests of planktic foraminifera were hand-picked from the >125µm fraction of sediments obtained by wet-sieving using tap water. A species with consistently high abundance, *Neogloboquadrina dutertrei*, was chosen in order to minimize differential abundance artifacts associated with bioturbation (Broecker et al., 1984). For the Eastern Equatorial Pacific the dominant foraminiferal species is *N. dutertrei* representing 60-70% of the Holocene and 45-65% of the last glacial foraminiferal assemblages (Martinez et al. 2006). This species prefers water depths of 60-150m, but shows a pronounced abundance peak between 25 and 50m in the Panama Basin (Fairbanks et al., 1982), and has $\delta^{18}O$ consistent with calcification from 50 to 100 m depth (Benway et al., 2006). In sample 15-20cm of core ME0005A-24JC and samples 11-18cm and 25-30cm of core Y69-71P, a second co-occurring species (*Globigerinoides sacculifer*) was analysed. The maximum concentrations of living *G. sacculifer* in the Panama Basin have been shown in 25-37m water depth (Fairbanks et al., 1982), while tracer analyses on shells from the sea floor suggest calcification depths of 30-40m (Benway et al., 2003).

For core ME0005A-24JC foraminiferal $^{14}C$ ages from 81cm, 230cm, 291cm and 351cm sediment depth used here are published in Kienast et al. (2007). The radiocarbon age from 120cm core depth in core Y69-71P is from Kish (2003).

### 3.3 Radiocarbon measurements

Samples were radiocarbon-dated at National Ocean Sciences Accelerator Mass Spectrometry (NOSAMS) Facility at Woods Hole Oceanographic Institution, USA and Leibniz-Laboratory Kiel, Germany (Table 3 in the Appendix). Samples for TOC-dating were submitted unprocessed, while alkenone samples were submitted as $CO_2$. For the conversion of purified alkenones into $CO_2$, the samples were transferred into pre-combusted quartz tubes and 150µg pre-combusted copper oxide (CuO) was added as an oxygen source. Using a vacuum line the samples were evacuated and flame-sealed.

Afterwards the samples were combusted at 900°C for 8 h, and resulting $CO_2$ was quantified and purified.

Foraminiferal samples measured at NOSAMS were submitted at dry shells, cleaned ultrasonically and with acid leaching of ~5-10% of the raw calcite. Foraminiferal samples measured at Leibniz-Laboratory were submitted as graphite. The foraminifera were cleaned with $H_2O_2$ and converted to $CO_2$ using phosphoric acid. The gas samples were furthermore purified and reduced to graphite with $H_2$ and using iron powder as a catalyst. AMS measurements of carbonate and TOC samples at NOSAMS were carried out using standard methods (McNichol et al., 1994). AMS measurements of alkenone isolates were performed following the protocol for small samples (Pearson et al., 1998).

Radiocarbon ages are reported as conventional radiocarbon ages ($\pm 1\sigma$ analytical error) referring to Stuiver and Polach (1977), which are corrected for carbon isotopic fractionation occurring during sample formation and processing. A conversion to calibrated (calendar) $^{14}C$ ages is not applied when discussing the age relationships of the samples. However, calibrated ages of foraminifera are used when sedimentation rates are calculated, or age models are developed. For calibration, the Marine04 calibration data set including a 400 years marine reservoir correction (Hughen et al., 2004) was applied using the calibration software CALIB 5.0.2 (Stuiver et al. 2005).

## 4. Results

### 4.1 ME0005A-24JC

The conventional $^{14}C$ ages of the dated sediment constituents (Table 2, Fig. 2) range from the Holocene to the Last Glacial Maximum (LGM). Radiocarbon ages of all sediment fractions increase with core depth (Figure 2). Measured radiocarbon ages of the planktic foraminifera, alkenones, and TOC agree well, generally within 400±100 $^{14}C$ years. This age offset is not significant (within 2σ analytical errors), especially considering the measurement uncertainties for small sample sizes (<300µg), which are related to sample preparation and combustion backgrounds as well as the analytical errors of AMS measurement. Here, we consider reported radiocarbon age offsets insignificant if they are within 2σ analytical uncertainties.

Alkenones are only up to 100±165 $^{14}C$ years older than foraminifera, except for the depth interval from 226.5 to 231.5cm where alkenones are 250±155 $^{14}C$ years younger than the foraminifera. Both values lie within 1σ error margins. TOC and alkenones also agree within 350±175 $^{14}C$ years. For the intervals 46-51cm and 76-81cm, only foraminifera and TOC $^{14}C$-data were obtained as the alkenone yields were too small to perform radiocarbon AMS measurements.

Overall, we conclude that the alkenones are not significantly pre-aged relative to other sediment constituents. TOC and foraminiferal ages show a maximum age offset of only 215±45 $^{14}C$ years. The sample from core depth 345-350cm represents an exception where TOC is 400±100 $^{14}C$ years younger than corresponding foraminifera. Taking into account that the foraminiferal age was measured from 351cm core depth, the actual age offset between TOC and foraminifera should be less pronounced and not significant.

### 4.2 Y69-71P

The $^{14}C$-dated core depths for core Y69-71P cover marine oxygen isotope stages 1 and 2 (Table 2, Fig. 3). All radiocarbon ages increase with core depth. Foraminifera and TOC ages agree within 355±70 $^{14}C$ years in most core depths. Exceptions are found at core depth 11-18cm (*G. sacculifer*) and 183-188cm (*N. dutertrei*) where TOC is 830±40 and 960±180 $^{14}C$ years older than foraminifera, respectively.

In most cases, we observe no systematic age offset between alkenones and TOC, which show age differences ranging from 80±140 to 800±255 $^{14}C$ years. Likewise, the age relationship between alkenones and foraminifera shows an inconsistent pattern with age offsets of 200±250 to 810±245 $^{14}C$ years.

Significant age offsets are evident for the depth interval 253-258cm, where TOC (23,700±130 $^{14}C$ yr BP) and alkenones (23,600±230 $^{14}C$ yr BP) are 3220±390 and 3320±435 $^{14}C$ years younger than corresponding foraminifera (26,920±370 $^{14}C$ yr BP). Furthermore, alkenone dates from near the core top (11-18cm and 25-30cm) are much older (up to 4530±330 $^{14}C$ years) than those of the other dated sediment components.

Alkenones and TOC differ by up to 3700±330 $^{14}$C years for the two uppermost depth intervals, and the former are 1240±270 to 4530±330 $^{14}$C years older than foraminifera for the 11-18cm and 25-30cm samples. The alkenones themselves show no significant age difference between 11-18cm and 25-30cm core depth. We consider these alkenone-radiocarbon ages to be less reliable due to very small sample sizes that were measured (<30µg C).

**4.3 MC16**

The dated core interval for core MC16 (Fig. 4, Table 2) spans the Holocene (<9000a BP). Foraminifera, alkenone and TOC $^{14}$C-ages agree to within a few hundred years, with a maximum age-offset of 670±95 $^{14}$C years. The core-top radiocarbon ages for the depth intervals 1-2cm and 3-4cm have different age relationships between the different sediment constituents. For 1-2cm, foraminifera (2240±35 $^{14}$C yr BP) are slightly older than TOC (2120±35 $^{14}$C years). In contrast, for 3-4cm the foraminifera are younger (1715±30 $^{14}$C yr BP) than corresponding TOC (2160±30 $^{14}$C yr BP). The alkenones (1810±85 $^{14}$C yr BP) were combined for the depth interval 0-4cm to yield enough material for radiocarbon dating. At 11-12cm core depth, all three sediment fractions agree to within 165±65 $^{14}$C years. The foraminifera at 31-32cm (8530±50 $^{14}$C yr BP) are slightly older than co-occurring alkenones (7860±80 $^{14}$C yr BP) and TOC (8040±45 $^{14}$C yr BP).

## 5. Discussion

Foraminifera are generally thought to most accurately represent the time of sediment deposition since their size and density are large enough to promote rapid sinking. This limits horizontal transport and lateral redistribution if bottom currents or tidal movements are weak. For the time intervals covered by our cores, these components are therefore in most cases considered the best estimate for the depositional age (uncorrected for reservoir or production effects).

In contrast, organic matter is associated with the fine grain-sized and low-density material, which may easily be incorporated into nepheloid layer aggregates, and become resuspended and laterally transported prior to final burial. Hence, age offsets between marine biomarkers or TOC and foraminifera can indicate supply of older organic material that has previously been stored elsewhere. One benefit of compound-specific radiocarbon dating of phytoplankton-derived biomarkers is that biases due to input of pre-aged terrigenous or ancient organic matter (e.g., from erosion of bedrock or fossil fuel derived contamination) can be excluded.

In most cases the reported $^{14}C$ ages of the different sediment constituents, i.e. alkenones, foraminifera and TOC, agree well in all studied cores (Figures 2-4). Therefore, the alkenone radiocarbon ages do not indicate significant or systematic inputs of pre-aged organic matter supplied via lateral sediment transport and redistribution. Likewise, the good agreement between the ages of marine planktic components (foraminifera and alkenones) and TOC excludes aged terrigenous material as a significant source of organic matter. The data do not preclude redistribution and lateral sediment transport, which is suggested by bulk and component sedimentation rates and $^{230}Th$ normalization. If redistribution is occurring, however, it must be dominated by resuspension of material from the benthic "fluff" layers of essentially zero age at the time of redeposition. This probably implies relatively local transport within the east-west trending troughs from which the cores were raised (Fig. 1), if any occurs.

$^{14}C$ age differences within $2\sigma$ error margins can in most cases be explained with measurement uncertainties. Sample preparation and chemical processing can introduce small amounts of carbon contaminant (carbon process blank) of unknown isotopic composition. This issue is especially critical for small sample sizes (<300µg) and compounds needing several processing steps like organic material. Nevertheless, small size alkenone purification in connection with $^{14}C$ dating at NOSAMS Facility is reliable within 17‰ or 500 $^{14}C$ years, respectively (Mollenhauer et al., 2005b, Ohkouchi et al., 2005b).

Some depth intervals show pronounced and significant age offsets. In core Y69-71P alkenones in the uppermost depth intervals (11-18cm and 25-30cm) are offset up to 3880±330 $^{14}C$ years to *N. dutertrei* and TOC, but notably, TOC and *N. dutertrei* ages agree within 180±40 $^{14}C$ years for depth interval 11-18cm. TOC is even 330±50 $^{14}C$

years younger than *N. dutertrei* in 25-30cm core depth. Conversely, in the oldest depth interval *N. dutertrei* is 3320±435 $^{14}$C years older than alkenones and TOC. The same pattern is evident in core MC16 at depth interval 30-32cm, where foraminiferal $^{14}$C ages are 670±95 and 490±65 $^{14}$C years older than alkenones and TOC, respectively. These age relationships between foraminifera, TOC and alkenones are less consistent and more muted than previously found (Mollenhauer et al., 2003; Ohkouchi et al., 2002). Lateral supply of pre-aged organic matter to the uppermost core section of Y69-71 is regarded less likely because of the good agreement between TOC and foraminiferal ages. Since TOC, mostly of marine origin, and alkenones reside in the same size fraction, they are expected to be affected by the same sedimentation processes. Thus, if lateral sediment transport occurred it should have also supplied other pre-aged marine organic matter resulting in higher TOC ages. Potential causes for the discrepancies thus include analytical biases during sample processing, organic matter degradation during core storage, bioturbation, calcification depth, differential dissolution, and selective transport of either the foraminiferal or organic fractions.

## 5.1 Potential biases of alkenone radiocarbon ages

### *5.1.1 Large blank contribution to small samples*

Age offsets of alkenones at 11-18cm and 25-30cm core depth in Y69-71P, which exceed 4500 $^{14}$C years, were measured from alkenone samples containing only 24 and 29µg carbon, respectively. Using isotopic mass balance equation we can calculate the amount of contamination required if the reported age offsets between alkenones and foraminifera were due to addition of blank carbon during sample processing alone. Assuming a contamination with $^{14}$C-dead material (fraction modern carbon *fMC*=0), approximately 38% or 43% blank C for depth interval 11-18cm would yield the observed age offset relative to co-occurring *N. dutertrei* or *G. sacculifer,* respectively. Assuming an fMC=0.25, the blank carbon would account for 60% (*N. dutertrei*) or 61% (*G. sacculifer*) of the measured sample. For core depth 25-30cm, the same calculation results in 14% or 39% (*N. dutertrei*) and 18% or 36% (*G. sacculifer*) blank C depending on whether an fMC value of 0 or 0.25 is used, respectively. This amount of contamination could have been introduced to the samples during any step of the sample preparation methodology. However, we consider addition of such large amounts of blank material unlikely, as $CO_2$ yields from combustion were close to the expected amount of carbon based on gas-chromatographic quantification of purified alkenones.

### *5.1.2 Degradation of alkenones during storage*

Core Y69-71P was retrieved in 1969 and had observed patches of surface mold when sampled. Selective bacterial degradation of alkenones can occur and the bacterial metabolic pathway includes isotopic fractionation during the degradation of alkenones to

alkenols (Gong and Hollander, 1999; Rontani et al., 2005; Rontani et al., 2008; Sun et al., 2004). However, if bacterial activity occurred, it is not expected to influence the radiocarbon content of the alkenones, since radiocarbon data reported according to Stuiver and Polach (1977) are corrected for isotopic fractionation during sample formation, decay as well as processing.

At present, we are unable to provide a satisfactory explanation for the unexpectedly old alkenones in the uppermost samples of Y69-71P. Unfortunately, sample availability does not permit us to repeat these measurements.

## 5.2 Potential biases on foraminiferal ages

For depth intervals 253-258cm of core Y69-71P and 30-32cm of core MC16 foraminiferal $^{14}C$ ages are significantly (>2σ analytical uncertainty) older than the other dated sediment constituents. If foraminiferal ages represent the best estimate of the time of deposition in locations affected by sediment transport we would not expect such an age relationship. Moreover, in previous studies, foraminifera were consistently reported to be the youngest sediment constituents (Mollenhauer et al., 2003; Mollenhauer et al., 2005a; Ohkouchi et al., 2002). Soxhlet and ASE extraction procedures seem not to introduce any significant uncertainties to the radiocarbon measurements of foraminiferal tests (Ohkouchi et al., 2005a). Likewise winnowing of the organic material, which is more susceptible to resuspension and transport, exposing relict foraminifera is unlikely. In addition to the above mentioned multiple lines of evidence for sediment focusing at the core sites, chirp subbottom profiler data for core Y69-71P (Lyle et al., 2005) show thick sediment coverage implying that the core was not taken at a location of sediment winnowing.

### *5.2.1 Bioturbation*

For core MC16 core-top radiocarbon ages are elevated and essentially constant down to 12cm sediment depth for all dated components. This pattern can be explained with bioturbation and is in agreement with the existing literature. Aller et al. (1998) report maximum bioturbation depths of up to 20cm for cores from the Northern Panama Basin.

A potential explanation for age offsets between the different components is age-dependent or particle size induced differential bioturbation by benthic organisms (Smith et al., 1993; Thomson et al., 1995). Mixing depths may be greater for fine than coarse grain sizes or younger than older material. This process, when coupled to different input abundance histories can induce complex phasing and smoothing effects in different grain-size fractions, especially where sedimentation rates are <10cm/kyr (Bard, 2001). However, differential bioturbation is an unlikely explanation for the age offsets observed at 253-258cm core depth of core Y69-71 showing >3000 $^{14}C$ years older foraminiferal

ages compared to co-occurring alkenones and TOC. The sedimentation rate of core Y69-71 ranges between 7 and 17cm/kyr (for 400cm core depth; Lyle et al., 2002). Lowest sedimentation rates are reconstructed for the interval from 8500 years to the core top, implying that those intervals may be more susceptible to bioturbation-induced offsets than glacial intervals. However, according to Bard (2001) bioturbation should in general not induce such a large age offset between different sediment constituents here.

For core MC16 with an estimated sedimentation rate of 2.7-3.1cm/kyr (using calibrated radiocarbon ages) an age offset of up to 2500 years induced by differential bioturbation would be expected according to Bard (2001; equation 1) assuming bioturbation depths of 15cm (fine fraction) and 5cm (coarse fraction). This offset is much higher than the observed $^{14}C$ age offset between foraminifera and organic matter ($\leq 670 \pm 95$ $^{14}C$ years).

*5.2.2 Calcification depth and differential dissolution of foraminiferal tests*

In the topmost core sections of core Y69-71P (11-18cm and 25-30cm) and core ME0005A-24JC (15-20cm) *G. sacculifer* is consistently younger than *N. dutertrei* by several hundred years. This finding is in line with the species-specific calcification depths in the euphotic zone, which are characterized by different DIC $^{14}C$ contents. However, the differences in calcification depth are small (Fairbanks et al., 1982), so observed age offsets are greater than would be expected for pre-anthropogenic DIC $^{14}C$ differences alone.

A possible explanation for $^{14}C$ age offsets between foraminiferal species introducing a bias towards younger ages might be differential dissolution in the sediment mixed layer (Barker et al., 2007), which can occur under the influence of carbonate ion undersaturated bottom waters, or as a result of respiratory $CO_2$ release in the sediment. In the Panama Basin, the lysocline depth was observed at around 2800m (Thunell et al., 1981), which is equivalent to the depths of our core sites ME0005A-24JC, Y69-71P and MC16. *G. sacculifer* is one of the most soluble species, whereas *N. dutertrei* is highly resistant (Berger, 1970). Thus differential dissolution of the more susceptible *G. sacculifer* could explain the younger radiocarbon ages of this species. Alternatively, differences in the species seasonal or interannual fluxes may contribute to the $^{14}C$ differences. *G. sacculifer* contains algal symbionts and can survive oligotrophic conditions during intervals of low upwelling, while *N. dutertrei* thrives during upwelling events, which bring deeper, relatively $^{14}C$-depleted, nutrient-rich water to the sea surface (Watkins et al., 1996). While there are no *G. sacculifer* ages for the core depth 253-258cm of core Y69-71P, published alkenone SST data (Kienast et al., 2006; Prahl et al., 2006), faunal assemblage changes (Martinez et al., 2006) and coupled $\delta^{18}O$, $\delta^{13}C$ and Mg/Ca SST data (Pena et al., 2008) do not suggest increased upwelling activity at our sites during the glacial interval, although stronger advection of cool waters upwelled into

the eastern boundary current off Peru and Chile is probable (Feldberg and Mix, 2003). We therefore regard this process to be of minor importance for the explanation of old foraminiferal tests in 253-258cm core depth.

*5.2.3 Addition of secondary calcite*

Secondary calcification could be a possible cause for the foraminiferal $^{14}C$ age of 253-258cm in Y69-71P. Secondary calcification within the sediment by precipitation of pore water DIC derived from old carbon from deeper sediments could be responsible for older $^{14}C$ ages of foraminifera (Barker et al., 2007). For an age offset of >3000 $^{14}C$ years, this requires the addition of large amounts of secondary calcite added to the foraminiferal tests. We can again use isotopic mass balance to calculate the amount of secondary calcite needed to cause the foraminiferal age offset. Assuming pore water DIC-addition from e.g. 15cm or 30cm deeper (fMC = 0.046 or 0.04 calculated with interpolated TOC-based sedimentation rate), the required additional amount of older calcite is 280% and 140%, respectively, which is implausible considering that only intact foraminifera without visual evidence of secondary calcite precipitation were handpicked for $^{14}C$ analysis.

*5.2.4 Downslope transport of foraminifera*

Downslope transport from nearby abyssal hills or the Carnegie Ridge is considered a possible explanation for older foraminiferal ages. As described above, between 85° and 86°W the central saddle of Carnegie Ridge shows an erosional valley, where incision into the acoustic basement from bottom water spillover is evident (Lonsdale, 1977; Van Andel et al., 1971). The Sand Dune Valley, located on the eastern side of this erosional feature, shows transverse dunes and barchans, which consist of sand-sized broken and intact Quaternary foraminiferal tests. The foraminiferal dunes are moved down-valley in a NW direction (towards our core locations) by the episodic spillover of bottom water across the central saddle of the Carnegie Ridge reaching velocities of >30cm/s (Lonsdale and Malfait, 1974). The eroded material is likely accumulated in abyssal valleys like our core sites. Since the process is episodic in nature, we do not expect large additions of fossil foraminifera in all core depths (and thus no important contribution to mass accumulation rates), which could explain that only one of our studied depths intervals seems to be affected. If this is the case, however, the fact that we did not find the same offsets in core ME0005A-24JC (closest to Carnegie Ridge) as we did in Y69-71P (one basin to the north) would have to be random chance.

Anomalously old foraminiferal $^{14}C$ ages of core MC16 (30-32cm) might be explained by downslope transport from the Malpelo Ridge, which is predominantly covered with carbonate from intact and broken foraminiferal tests. But sediment winnowing from the Malpelo Ridge may be less extensive since the concentration of more

readily mobilizable fine-grained carbonate on the Malpelo Ridge is higher than on the Carnegie Ridge (Moore et al., 1973).

### 5.3 Potential particle sources and timescales of lateral transport

Despite potential radiocarbon age biases related to the above mentioned processes, all sediment constituents agree well in age in most of the core depths of cores ME0005-24JC, Y69-71P and MC16 and thus sediment redistribution likely occurs syn-depositionally. For our study area, especially for cores ME0005A-24JC and Y69-71P, the syn-depositionally transported sedimentary material is probably derived from nearby abyssal hills by interaction with abyssal tidal flow (internal tides). Enhanced current velocities near the seafloor may enhance the small scale vertical shear and thereby increase the probability of sediment erosion and redistribution. The resuspended sediment is injected into the near-bottom water, where it is laterally displaced away from the topographical highs (Turnewitsch et al., 2008). This is in agreement with the $^{230}Th_{xs}$ data from Kienast et al. (2007), as the supplied material is likely to have been transported by bottom currents, according to the basic assumptions of the $^{230}Th$ normalization method (Francois et al., 2004). Based on modeling studies, Egbert et al. (2004) reconstructed the tidal kinetic energy and tidal dissipation in the deep ocean for the LGM. Their results show enhanced global tidal dissipation during the LGM compared to present day conditions, especially in the deep ocean. This way, enhanced lateral transport could explain high sediment focusing factors in the Panama Basin during the last glacial. Nevertheless, internal tides do also occur in the Holocene and could have contributed to the apparent sediment focusing, even though they were weaker than during the LGM (Kienast et al., 2007).

Honjo et al. (1992) present data for the northern Panama Basin, which give evidence for strongest deep currents in approximately 2000m water depth. This is in good agreement with our assumption that the resuspended material derives from the topographic highs around our locations, which rise to approximately 2300-1800m water depth (Fig. 1B). Likewise, the measured current velocities (on average 5-7cm/s) are in the range needed to resuspend low-density material (organic matter), but to not affect denser material like foraminifera.

Considering the minor age offsets of the radiocarbon-dated sediment constituents in most of the samples of cores ME0005A-24JC, Y69-71P and MC16, the apparent lack of aged terrigenous organic matter, and the $^{230}Th_{xs}$ derived focusing factors of Kienast et al. (2007), we suggest that laterally supplied material is rapidly transported and redistributed by bottom currents soon after particle formation or particle sedimentation. Using $^{234}Th/^{238}U$ disequilibria, Turnewitsch et al. (2008) calculated residence times of laterally transported particulate matter resuspended from a sloping seafloor by internal tides. The residence time of those particles in near-bottom water traced by $^{234}Th$ is <2-3

weeks. This is consistent with sediment redistribution on a local scale. However, this residence time might significantly increase by further interaction with the kilometer-scale topography, but the overall magnitude is most probably below the analytical uncertainties associated with radiocarbon dating.

Furthermore, $U_{37}^{k'}$ (alkenone unsaturation index) derived sea surface temperatures (SST) of cores ME0005-24JC (Kienast et al., 2006) and Y69-71P (Prahl et al., 2006) and our own data (Appendix) agree in the topmost samples (late Holocene) with annual mean SSTs at this site (Locarnini et al., 2006). This argues against transport processes over long distances, since the $U_{37}^{k'}$ index would reflect the SST signal of the region of the alkenone origin (Benthien and Müller, 2000; Mollenhauer et al., 2006; Ohkouchi et al., 2002).

Moreover, cores ME0005-24JC and Y69-71P (Fig. 1) as well as core MC16 (not shown) are located in narrow east-west trending troughs, which are bordered by the Carnegie Ridge in the south and the Cocos-Nazca Rise in the north. This surrounding large-scale topography restricts the potential source regions for bottom current driven advection and supports the assumption that laterally transported material is mainly derived from nearby topographic highs within the east-west trending troughs. Contrary, the supply of pre-aged foraminifera from the Carnegie Ridge (at ~130km from the core sites) might be triggered by a yet unknown but different mechanism than tidal dissipation. Since the sediments of its northern flank consist of relict foraminiferal sands, high concentrations of old alkenones are not expected at this erosional site. Modern alkenones from the overlying water column would, however, not affect the $U_{37}^{k'}$ based SST estimate as they would reflect conditions similar to those alkenones synthesized at our core sites ($\Delta$SST <0.7°C; Locarnini et al., 2006). However, old foraminiferal tests would record Mg/Ca SST from the time of synthesis. Significant disagreements between the $U_{37}^{k'}$ exist in early Holocene, deglacial and glacial intervals of these cores, however. The origin of these differences is not known, but is under consideration (Prahl and Kienast, personal communication 2009). Our radiocarbon data constrain these considerations and exclude the possibility that offsets in $U_{37}^{k'}$ between these cores reflects differential input of older materials.

For core MC16 our $^{14}C$ data do not necessarily imply resuspension and redistribution of organic matter. Nevertheless, this location is influenced by the bottom water circulation of the Panama Basin (Figure 1), and is situated just south of the Malpelo Ridge, which is mostly covered with fine-grained sediments that may serve as a source of advected sediment (Druffel et al., 1998; Moore et al., 1973; Van Andel, 1973). For core P7, which is located in the Central Panama Basin NW of core MC16 in a similar water depth, Kienast et al. (2007) measured slightly elevated recent $^{230}Th_{xs}$ levels and

calculated higher focusing for the glacial. If we assume that cores P7 and MC16 are influenced by a similar sediment depositional pattern, it is likely that MC16 is also influenced by lateral advection of sediments. Our $^{14}C$ results, which mostly show insignificant age differences between alkenones, foraminifera and TOC, indicate that like for cores ME0005A-24JC and Y69-71P, the timescale for lateral transport is rapid and occurs syndepostionally, i.e. less than a few decades after particle formation and synchronous within the uncertainty associated with the radiocarbon method. As the $U_{37}^{k'}$ derived SST (not shown) also matches the mean annual temperature at this site (WOA 2005), we consider the advection processes to also occur on a local (trough-wide) scale.

**5.4 Implications for paleoceanographic studies in the southern Panama Basin**

Paleoceanographic studies reconstructing marine productivity and vertical carbon export using accumulation rates of different sedimentary constituents have shown higher glacial export rates compared to interglacials (Lyle et al., 2002; Paytan et al., 1996; Sarnthein et al., 1988). Contrary results were obtained in studies using constant flux proxies (Kienast et al. 2007; Loubere, 1999; Loubere, 2000; Loubere et al., 2003; Loubere et al., 2004) and faunal assemblages (Loubere, 1999; Martinez et al., 2006) implying reduced glacial productivity and enhanced sediment focusing. In light of this paradox, the applicability of the $^{230}Th$ method in the in the Panama Basin is controversial (Broecker, 2008; Francois et al., 2007; Kienast et al., 2007; Lyle et al., 2005; Lyle et al., 2007; Siddall et al., 2008).

Our results have important implications for these paleoceanographic studies. Since the age discrepancy between the different sediment components is small and the transported material is likely to be advected from nearby topography the rapid sediment transport processes within the Panama Basin do not lead to a decoupling of proxy records residing in different grain size fractions. Therefore, combined records of paleoproxies from different grain-size fractions as presented by Kienast et al. (2006) and Prahl et al. (2006) can indeed be considered coeval in this region. For example, apparent offsets between paleotemperatures estimated from $U_{37}^{k'}$ and those estimated from Mg/Ca ratios in foraminifera cannot be dismissed as artifacts of local reworking, but must be explained based on environmental influences on the respective proxies (Mix, 2006). However, one aspect revealed by our study is the potential selective transport of foraminiferal sands washed downslope from the Carnegie Ridge, which might bias paleoceanographic reconstructions based on foraminiferal tests. Our results suggest the occurrence of episodic downslope transport particularly for the glacial time period. The unexpectedly old *N. dutertrei* in core depth 253-258cm and the deviation of foraminiferal $^{14}C$ ages from Clark et al. (2004) with our data of core Y69-71P furthermore suggests that the age model for this core used in Kienast et al. (2007) might need to be revised. This implies

that $^{230}$Th derived focusing factors would even increase for marine oxygen isotope stage 2 time interval used in Kienast et al. (2007).

Irrespective of which of the mechanisms suggested to affect $^{230}Th_{xs}$ inventories (i.e. lateral redistribution or water column scavenging, or any other yet unknown influence) is the true controlling process, our data give strong evidence for a local (trough-wide) source of all marine sediment constituents. Evidence for delivery of distant marine organic matter or addition of any pre-aged terrigenous components supplied from the continental margins or by dust is lacking.

## 6. Summary and Conclusion

Radiocarbon ages of alkenones, foraminifera and TOC in most core depths of cores ME0005A-24JC, Y69-71P and MC16 have insignificant $^{14}C$ age offsets between the different sediment components, arguing against long-distance lateral supply and deposition of pre-aged allochthonous material from marine or terrestrial sources in the Panama Basin. This finding constrains mechanisms of sediment focusing inferred from $^{230}Th_{xs}$ data (Kienast et al., 2007).

Allochthonous material in this region likely stems from local particle winnowing from kilometer-scale topographic highs within the east-west trending troughs by internal tidal activity or bottom currents that return recently sedimented particles to bottom waters. These tidal water movements or bottom currents locally transports and redistributes the particles within less than a few decades after particle formation, equal to the uncertainty of the radiocarbon method.

Spillover of fast bottom currents originating in the Peru Basin and crossing the Carnegie Ridge may occur episodically, transporting coarser-grained particles downslope to the Southern Panama Basin. A bias in paleoceanographic reconstructions based on foraminiferal tests for core Y69-71P might arise from this process, although it is not obvious why similar effects would not have been found in core ME0005A-24JC which is closer to Carnegie Ridge and in slightly deeper water.

The proximity and rapidity of transport precludes extensive alteration of the entrained pelagic organic matter. Enhanced tidally related current velocites in the abyssal ocean during lowstands of sea level may explain higher sediment focusing factors found in the Panama Basin during glacial time compared to the Holocene.

**Acknowledgments**

This study was funded by the Helmholtz Young Investigators Group „Applications of molecular $^{14}C$ analysis for the study of sedimentation processes and carbon cycling in marine sediments". We kindly thank Ralph Kreutz and Daniel Montluçon for laboratory assistance, Birgit Meyer-Schack and Monika Segl for $^{14}C$ processing guidance. G.M. acknowledges financial support from WHOI postdoctoral scholarship program. T.I.E. was supported by NSF grant OCE-0526268. A.C.M. was supported by NSF grant ATM0602395. We thank R. Turnewitsch, two anonymous reviewers and M.L. Delaney (editor) for beneficial comments that improved this manuscript.

**References**


Aller, R.C., Hall, P.O.J., Rude, P.D., Aller, J.Y., 1998. Biogeochemical heterogeneity and suboxic diagenesis in hemipelagic sediments of the Panama Basin. Deep Sea Research Part I: Oceanographic Research Papers. 45, 133-165.

Asper, V.L., Honjo, S., Orsi, T.H., 1992. Distribution and transport of marine snow aggregates in the Panama Basin. Deep Sea Research Part A. Oceanographic Research Papers. 39, 939-952.

Bard, E., 2001. Paleoceanographic implications of the difference in deep-sea sediment mixing between large and fine particles. Paleoceanography. 16, 235-239.

Barker, S., Broecker, W.S., Clark, E., Hajdas, I., 2007. Radiocarbon age offsets of foraminifera resulting from differential dissolution and fragmentation within the sedimentary bioturbated zone. Paleoceanography. 22, PA2205, doi:10.1029/2006PA001354

Beaulieu, S.E., 2002. Accumulation and fate of phytodetritus on the sea floor. Oceangraphy and Marine Biology: an annual review. 40, 171-232.

Behrenfeld, M. J., Bale, A. J., Kolber, Z. S., Aiken, J., Falkowski, P. G. 1996. Confirmation of iron limitation of phytoplankton photosynthesis in the equatorial Pacific Ocean. Nature. 383, 508-511.

Behrenfeld, M.J., Falkowski, P.G., 1997. Photosynthetic rates derived from satellite-based chlorophyll concentration. Limnology and Oceanography. 42, 1-20.

Benthien, A., Müller, P.J., 2000. Anomalously low alkenone temperatures caused by lateral particle and sediment transport in the Malvinas Current region, western Argentine Basin. Deep Sea Research Part I: Oceanographic Research Papers. 47, 2369-2393.

Benway, H.M., Haley, B.A., Klinkhammer G.P., Mix, A.C., 2003. Adaptation of a Flow-Through Leaching Procedure for Mg/Ca Paleothermometry. Geochemistry, Geophysics, Geosystems. 4, 1-15.

Benway, H.M., Mix, A.C., Haley, B.A., Klinkhammer, G.P., 2006. Eastern Pacific Warm Pool paleosalinity and climate variability: 0-30 ky. Paleoceanography. 21, PA3008, doi: 10.1029/2005PA001208.

Berger, W.H., 1970. Planktonic Foraminifera: Selective solution and the lysocline. Marine Geology. 8, 111-138.

Broecker, W. S., Mix, A. C. Andree, M., Oeschger, H., 1984. Radiocarbon measurements on co-existing benthic and planktonic foraminiferal shells: Potential for reconstructing ocean ventilation times over the past 20,000 years. Nuclear Instruments and methods in Physics Research. B5, 335-339.

Broecker, W.S., 2008. Excess sediment $^{230}$Th: Transport along the sea floor or enhanced water column scavenging? Global Biogeochemical Cycles. 22, GB1006, doi:10.1029/2007GB003057.

Chavez, F.P., Barber, R.T., 1987. An estimate of new production in the equatorial Pacific. Deep Sea Research Part A. Oceanographic Research Papers. 34, 1229-1243.

Clark, P.U., McCabe, A.M., Mix, A.C., Weaver, A.J., 2004. Rapid Rise of Sea Level 19,000 Years Ago and Its Global Implications. Science. 304, 1141-1144.

Druffel, E.R.M., Griffin, S., Honjo, S., Manganini, S.J., 1998. Evidence of Old Carbon in the Deep Water Column of the Panama Basin from Natural Radiocarbon Measurements. Geophysical Research Letters. 25, 1733-1736.

Egbert, G.D., Ray, R.D., Bills, B.G., 2004. Numerical modeling of the global semidiurnal tide in the present day and in the last glacial maximum. J. Geophys. Res. 109, C03003, 10.1029/2003JC001973.

Fairbanks, R.G., Sverdlove, M., Free, R., Wiebe, P.H., Be, A.W.H., 1982. Vertical distribution and isotopic fractionation of living planktonic foraminifera from the Panama Basin. Nature. 298, 841-844.

Feldberg, M.J., Mix, A.C. (2003) Planktonic foraminifera, sea-surface temperatures, and mechanisms of oceanic change in the Peru and South Equatorial Currents, 0-150 ka BP. Paleoceanography. 18, PA1016, doi:10.1029/2001PA000740.

Francois, R., Frank, M., Rutgers van der Loeff, M., M., Bacon, M., P., 2004. $^{230}$Th normalization: An essential tool for interpreting sedimentary fluxes during the late Quaternary. Paleoceanography. 19, PA1018, doi:10.1029/2003PA000939.

Francois, R., Frank, M., Rutgers van der Loeff, M., Bacon, M.P., Geibert, W., Kienast, S., Anderson, R.F., Bradtmiller, L., Chase, Z., Henderson, G., Marcantonio, F., Allen, S.E., 2007. Comment on ''Do geochemical estimates of sediment focusing pass the sediment test in the equatorial Pacific?'' by M. Lyle et al. Paleoceanography. 22, PA1216, doi:10.1029/2005PA001235.

Gong, C., Hollander, D.J., 1999. Evidence for differential degradation of alkenones under contrasting bottom water oxygen conditions: implication for paleotemperature reconstruction. Geochimica et Cosmochimica Acta. 63, 405-411.

Honjo, S., 1982. Seasonality and Interaction of Biogenic and Lithogenic Particulate Flux at the Panama Basin. Science. 218, 883-884.

Honjo, S., Spencer, D.W., Farrington, J.W., 1982. Deep Advective Transport of Lithogenic Particles in Panama Basin. Science. 216, 516-518.

Honjo, S., Spencer, D.W., Gardner, W.D., 1992. A sediment trap intercomparison experiment in the Panama Basin, 1979. Deep Sea Research Part A. Oceanographic Research Papers. 39, 333-358.

Hughen, K.A., Baillie, M.G.L., Bard, E., Beck, J.W., Bertrand, C.J.H., Blackwell, P.G., Buck, C.E., Burr, G.S., Cutler, K.B., Damon, P.E., Edwards, R.L., Fairbanks, R.G., Friedrich, M., Guilderson, T.P., Kromer, B., McCormac, G., Manning, S., Ramsey, C.B., Reimer, P.J., Reimer, R.W., Remmele, S., Southon, J.R., Stuiver, M., Talamo, S., Taylor, F.W., van der Plicht, J., Weyhenmeyer, C.E., 2004. Marine04 Marine Radiocarbon Age Calibration, 0–26 Cal Kyr BP. Radiocarbon. 46, 1059-1086.

Kessler, W.S., 2006. The circulation of the eastern tropical Pacific: A review. Progress In Oceanography. 69, 181-217.

Kienast, M., Kienast, S.S., Calvert, S.E., Eglinton, T.I., Mollenhauer, G., Francois, R., Mix, A.C., 2006. Eastern Pacific cooling and Atlantic overturning circulation during the last deglaciation. Nature. 443, 846-849.

Kienast, S.S., Kienast, M., Mix, A.C., Calvert, S.E., Francois, R., 2007. Thorium-230 normalized particle flux and sediment focusing in the Panama Basin region during the last 30,000 years. Paleoceanography. 22, PA 2213, doi:10.1029/2006PA001357.

Kish, S., 2003. Changing Export Production in the Eastern Equatorial Pacific, 160 ka to Present, Unpublished MS Thesis, Oregon State University, 86pp.

Kolber, Z. S., Barber, R. T. Coale, K. H., Fitzwateri, S. E., Greene, R. M., Johnson, K. S., Lindley, S., Falkowski, P. G., 1994. Iron limitation of phytoplankton photosynthesis in the equatorial Pacific Ocean. Nature. 371, 145-149.

Laird, N.P., 1971. Panama Basin Deep Water - Properties and Circulation. Journal of Marine Research. 29, 226-234.

Locarnini, R.A., Mishonov, A.V., Antonov, J.I., Boyer, T.P., Garcia, H.E., 2006. World Ocean Atlas 2005, Volume 1: Temperature. S. Levitus, Ed. NOAA Atlas NESDIS 61, U.S. Government Printing Office, Washington, D.C., 182 pp.

Lonsdale, P., 1977. Inflow of bottom water to the Panama Basin. Deep Sea Research. 24, 1065-1094.

Lonsdale, P., Malfait, B., 1974. Abyssal Dunes of Foraminiferal Sand on the Carnegie Ridge. Bulletin of the Geological Society of America. 85, 1697-1712.

Loubere, P., 1999. A multiproxy reconstruction of biological productivity and oceanography in the eastern equatorial Pacific for the past 30,000 years. Marine Micropaleontology. 37, 173-198.

Loubere, P., 2000. Marine control of biological production in the eastern equatorial Pacific Ocean. Nature. 406, 497-500.

Loubere, P., Fariduddin, M., Murray, R.W., 2003. Patterns of export production in the eastern equatorial Pacific over the past 130,000 years. Paleoceanography. 18, PA1028, doi:10.1029/2001PA000658.

Loubere, P., Mekik, F., Francois, R., Pichat, S., 2004. Export fluxes of calcite in the eastern equatorial Pacific from the Last Glacial Maximum to present. Paleoceanography. 19, PA2018, doi:10.1029/2003PA000986.

Loubere, P., Richaud, M., 2007. Some reconciliation of glacial-interglacial calcite flux reconstructions for the eastern equatorial Pacific. Geochemistry Geophysics Geosystems. 8, Q03008, doi:10.1029/2006GC001367.

Lyle, M., Mix, A., Pisias, N., 2002. Patterns of $CaCO_3$ deposition in the eastern tropical Pacific Ocean for the last 150 kyr: Evidence for a southeast Pacific depositional spike during marine isotope stage (MIS) 2. Paleoceanography. 17, 1013, doi:1010.1029/2000PA000538.

Lyle, M., N., M., Pisias, N., Mix, A., Martinez, J.I., Paytan, A., 2005. Do geochemical estimates of sediment focusing pass the sediment test in the equatorial Pacific? Paleoceanography. 20, PA1005, doi:10.1029/2004PA001019.

Lyle, M., Pisias, N., Paytan, A., Martinez, J.I., Mix, A., 2007. Reply to comment by R. Francois et al. on "Do geochemical estimates of sediment focusing pass the sediment test in the equatorial Pacific?": Further explorations of $^{230}Th$ normalization. Paleoceanography. 22, PA1217, doi:10.1029/2006PA001373.

Malfait, B.T., Van Andel, T.H., 1980. A modern oceanic hardground on the Carnegie Ridge in the eastern Equatorial Pacific. Sedimentology. 27, 467-496.

Marcantonio, F., Anderson, R.F., Higgins, S., Stute, M., Schlosser, P., Kubik, P., 2001. Sediment focusing in the central equatorial Pacific Ocean. Paleoceanography. 16, 260-267.

Marlowe, I.T., Brassell, S.C., Eglinton, G., Green, J.C., 1984. Long chain unsaturated ketones and esters in living algae and marine sediments. Organic Geochemistry. 6, 135-141.

Martinez, I., Rincon, D., Yokoyama, Y., Barrows, T., 2006. Foraminifera and coccolithophorid assemblage changes in the Panama Basin during the last deglaciation: Response to sea-surface productivity induced by a transient climate change. Palaeogeography, Palaeoclimatology, Palaeoecology. 234, 114-126.

Mix, A.C., 2006. Running hot and cold in the eastern equatorial Pacific. Quaternary Science Reviews. 25, 1147-1149.

McNichol, A.P., Osborne, E.A., Gagnon, A.R., Fry, B., Jones, G.A., 1994. TIC, TOC, DIC, DOC, PIC, POC -- unique aspects in the preparation of oceanographic samples for $^{14}C$-AMS. Nuclear Instruments and Methods in Physics Research Section B: Beam Interactions with Materials and Atoms. 92, 162-165.

Mollenhauer, G., Eglinton, T.I., Ohkouchi, N., Schneider, R.R., Muller, P.J., Grootes, P.M., Rullkotter, J., 2003. Asynchronous alkenone and foraminifera records from the Benguela Upwelling System. Geochimica et Cosmochimica Acta. 67, 2157-2171.

Mollenhauer, G., Kienast, M., Lamy, F., Meggers, H., Schneider, R.R., Hayes, J.M., Eglington, T.I., 2005. An evaluation of $^{14}C$ age relationships between co-occurring foraminifera, alkenones, and total organic carbon in continental margin sediments. Paleoceanography. 20, PA1016, doi:10.1029/2004PA001103.

Mollenhauer, G., McManus, J.F., Benthien, A., Muller, P.J., Eglinton, T.I., 2006. Rapid lateral particle transport in the Argentine Basin: Molecular $^{14}C$ and $^{230}Th_{xs}$ evidence. Deep Sea Research Part I: Oceanographic Research Papers. 53, 1224-1243.

Mollenhauer, G., Montlucon, D., Eglinton, T.I., 2005. Radiocarbon Dating of Alkenones from Marine Sediments: II. Assessment of Carbon Process Blanks. Radiocarbon. 47, 413-424.

Moore, T.C., Jr., Heath, G.R., Kowsmann, R.O., 1973. Biogenic sediments of the Panama Basin. Journal of Geology. 81, 458-472.

Ohkouchi, N., Eglinton, T.I., Hughen, K.A., Roosen, E., Keigwin, L.D., 2005. Radiocarbon Dating of Alkenones from Marine Sediments: III. Influence of Solvent Extraction Procedures on $^{14}C$ Measurements of Foraminifera. Radiocarbon. 47, 425-432.

Ohkouchi, N., Eglinton, T.I., Keigwin, L.D., Hayes, J.M., 2002. Spatial and Temporal Offsets Between Proxy Records in a Sediment Drift. Science. 298, 124-1227.

Ohkouchi, N., Xu, L., Reddy, C.M., Montlucon, D., Eglinton, T.I., 2005. Radiocarbon Dating of Alkenones from Marine Sediments: I. Isolation Protocol. Radiocarbon. 47, 401-412.

Paytan, A., Kastner, M., Chavez, F.P., 1996. Glacial to Interglacial Fluctuations in Productivity in the Equatorial Pacific as Indicated by Marine Barite. Science. 274, 1355-1357.

Pearson, A., McNichol, A.P., Schneider, R.J., Reden, K.F.v., Zheng, Y., 1998. Microscale AMS $^{14}C$ measurement at NOSAMS. Radiocarbon. 40, 61-75.

Pedersen, T.F., 1983. Increased productivity in the eastern equatorial Pacific during the last glacial maximum (19,000 to 14,000 yr B.P.). Geology. 11, 16-19.

Pena, L. D., Cacho, I., Ferretti, P., Hall M. A., 2008. El Niño–Southern Oscillation–like variability during glacial terminations and interlatitudinal teleconnections. Paleoceanography. 23, PA3101, doi:10.1029/2008PA001620.

Pennington, J.T., Mahoney, K.L., Kuwahara, V.S., Kolber, D.D., Calienes, R., Chavez, F.P., 2006. Primary production in the eastern tropical Pacific: A review. Progress In Oceanography. 69, 285-317.

Pisias, N.G., Mix, A.C., 1997. Spatial and Temporal Oceanographic Variability of the Eastern Equatorial Pacific During the Late Pleistocene: Evidence from Radiolaria Microfossils. Paleoceanography. 12, 381-393.

Prahl, F.G., Mix, A.C., Sparrow, M.A., 2006. Alkenone paleothermometry: Biological lessons from marine sediment records off western South America. Geochimica et Cosmochimica Acta. 70, 101-117.

Rontani, J.-F., Bonin, P., Jameson, I., Volkman, J.K., 2005. Degradation of alkenones and related compounds during oxic and anoxic incubation of the marine haptophyte Emiliania huxleyi with bacterial consortia isolated from microbial mats from the Camargue, France. Organic Geochemistry. 36, 603-618.

Rontani, J.-F., Harji, R., Guasco, S., Prahl, F.G., Volkman, J.K., Bhosle, N.B., Bonin, P., 2008. Degradation of alkenones by aerobic heterotrophic bacteria: Selective or not. Organic Geochemistry. 39, 34-51.

Rühlemann, C., Butzin, M., 2006. Alkenone temperature anomalies in the Brazil-Malvinas Confluence area caused by lateral advection of suspended particulate material. Geochem. Geophys. Geosyst. 7, Q10015, doi:10.1029/2006GC001251.

Sarnthein, M., Winn, K., Duplessy, J.C., Fontugne, M.R., 1988. Global Variations of Surface Ocean Productivity in Low and Mid Latitudes: Influence on $CO_2$ Reservoirs of the Deep Ocean and Atmosphere During the Last 21,000 Years. Paleoceanography. 3, 361-399.

Siddall, M., Anderson, R.F., Winckler, G., Henderson, G.M., Bradtmiller, L.I., McGee, D., Franzese, A., Stocker, T.F., Müller, S.A., 2008. Modeling the particle flux effect on distribution of $^{230}$Th in the equatorial Pacific. Paleoceanography. 23, 2208, doi:10.1029/2007PA001556.

Smith, C. R., Pope, R. H., DeMaster, D. J., Magaard, L., 1993. Age-dependent mixing of deep-sea sediments. Geochimica et Cosmochimica Acta. 57, 1473-1488.

Stuiver, M., Polach, H.A., 1977. Reporting of $^{14}$C Data. Radiocarbon. 19, 355-363.

Stuiver M., Reimer P. J. and Reimer R., 2005. CALIB - radiocarbon calibration, version 5.0.2 (http://calib.qub.ac.uk/calib/).

Sun, M.-Y., Zou, L., Dai, J., Ding, H., Culp, R.A., Scranton, M.I., 2004. Molecular carbon isotopic fractionation of algal lipids during decomposition in natural oxic and anoxic seawaters. Organic Geochemistry. 35, 895-908.

Thomsen, L., Gust, G., 2000. Sediment erosion thresholds and characteristics of resuspended aggregates on the western European continental margin. Deep Sea Research Part I: Oceanographic Research Papers. 47, 1881-1897.

Thomson, J., Cook, G.T., Anderson, R., MacKenzie, A.B., Harkness, D.D., McCave, I.N., 1995. Radiocarbon age offsets in different-sized carbonate components of deep-sea sediments. Radiocarbon. 37, 91-101.

Thunell, R.C., Keir, R.S., Honjo, S., 1981. Calcite Dissolution: An in situ Study in the Panama Basin. Science. 212, 659-661.

Turnewitsch, R., Reyss, J.-L., Nycander, J., Waniek, J.J., Lampitt, R.S., 2008. Internal tides and sediment dynamics in the deep sea--Evidence from radioactive $^{234}$Th/$^{238}$U disequilibria. Deep Sea Research Part I: Oceanographic Research Papers. 55, 1727-1747.

Van Andel, T.H., 1973. Texture and dispersal of sediments in the Panama Basin. Journal of Geology. 81, 434-457.

Van Andel, T.H., Ross Heath, G., Malfait, B.T., Heinrichs, D.F., Ewing, J.I., 1971. Tectonics of the Panama Basin, Eastern Equatorial Pacific. Geological Society of America Bulletin. 82, 1489-1508.

Watkins, J.M., A.C. Mix, Wilson, J., 1996. Living Planktic Foraminifera: Tracers of circulation and productivity in the central equatorial Pacific. Deep-Sea Research II. 43, 1257-1282.
Wyrtki, K., 1967. Circulation and Water Masses in the Eastern Equatorial Pacific Ocean. International Journal of Oceanology and Limnology. 1, 117-147.
Ziervogel, K., Bohling, B., 2003. Sedimentological parameters and erosion behaviour of submarine coastal sediments in the south-western Baltic Sea. Geo-Marine Letters. 23, 43-52.

Figures

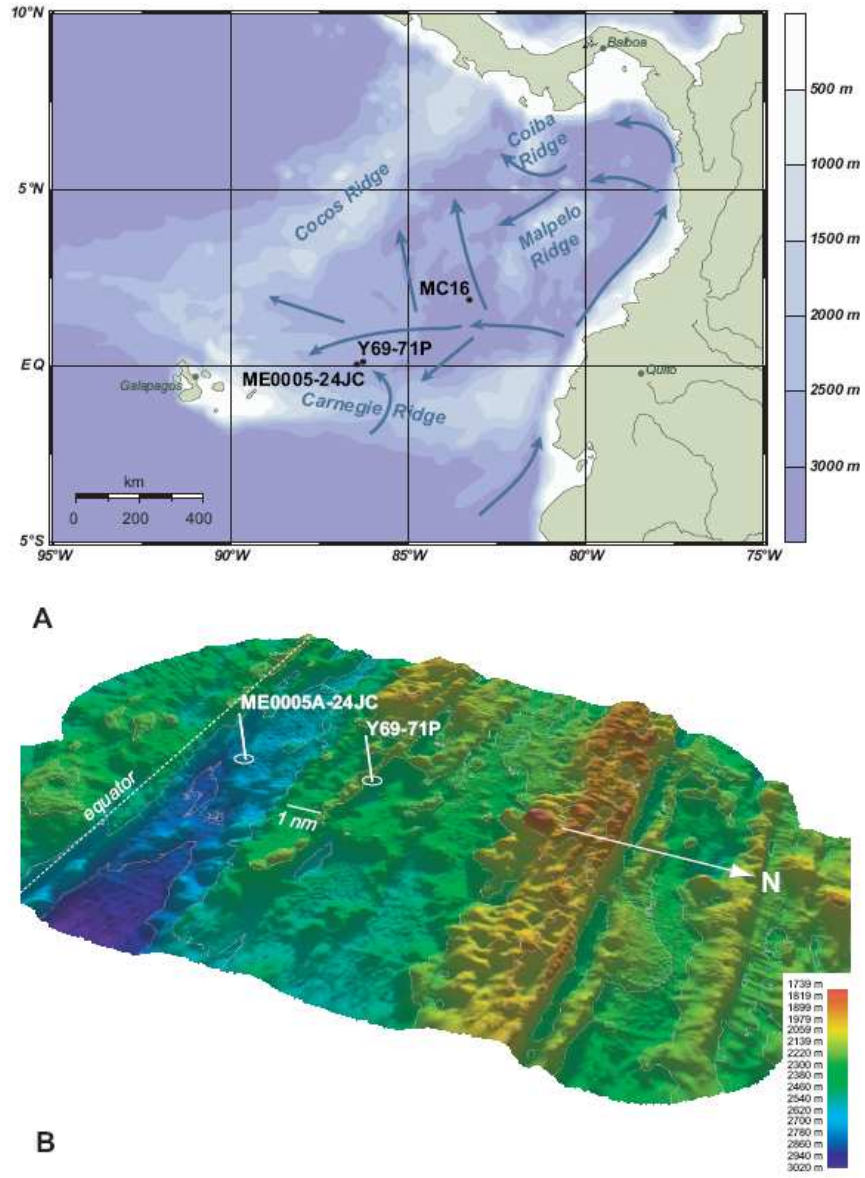


Figure 1. A) Study area and core locations. Grey arrows indicate flow directions of bottom currents. B) High resolution swath bathymetry image showing the abyssal hill topography around cores ME0005A-24JC and Y69-71P. Note east-west trending troughs.

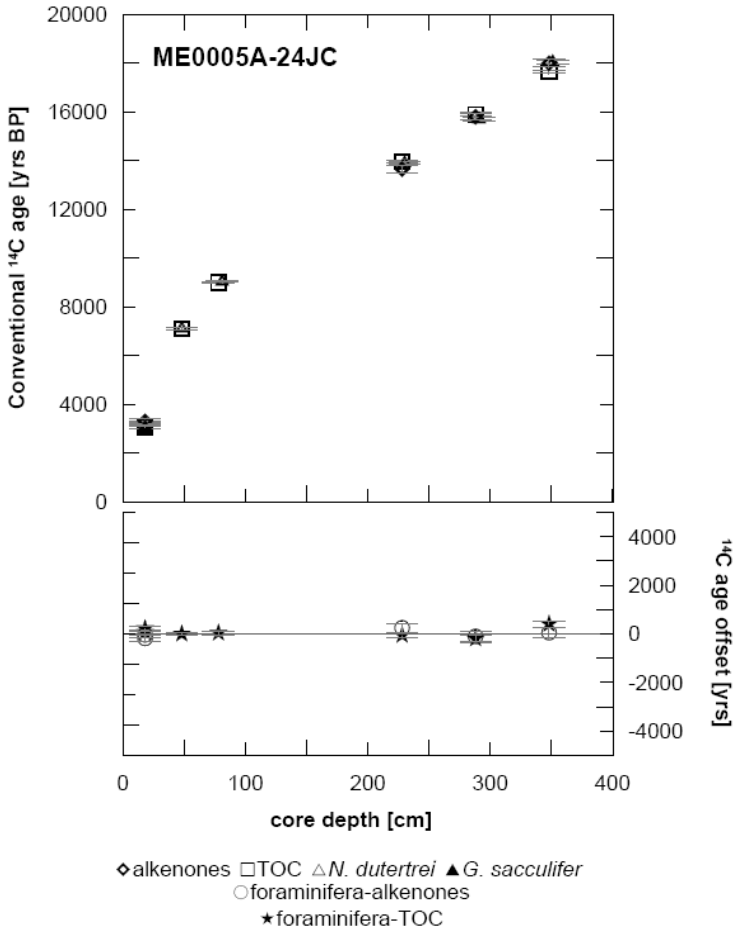


Figure 2. Conventional radiocarbon ages of alkenones, foraminifera (N. dutertrei and G. sacculifer) and Total Organic Carbon (TOC) for core ME0005A-24JC and the age-offsets between alkenones and foraminifera (open circles) and TOC and foraminifera (stars). Error bars indicate 1σ analytical uncertainty (the propagated error is given in the lower panel).

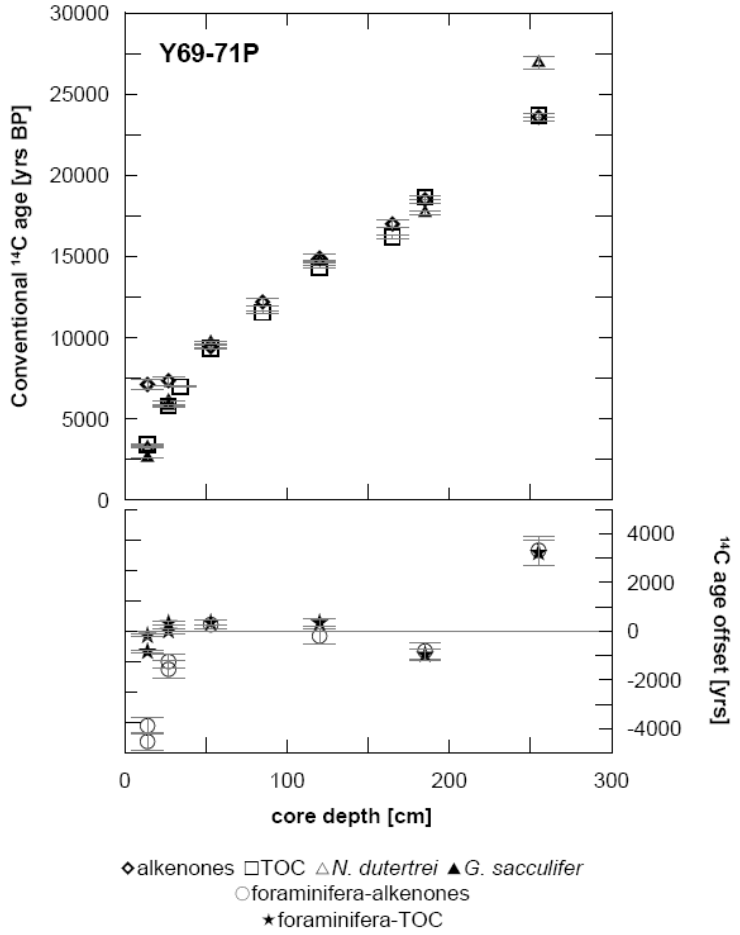


Figure 3. Conventional radiocarbon ages of alkenones, foraminifera (N. dutertrei and G. sacculifer) and Total Organic Carbon (TOC) for core Y69-71P and the age-offsets between alkenones and foraminifera (open circles) and TOC and foraminifera (stars). Error bars indicate 1σ analytical uncertainty (the propagated error is given in the lower panel).

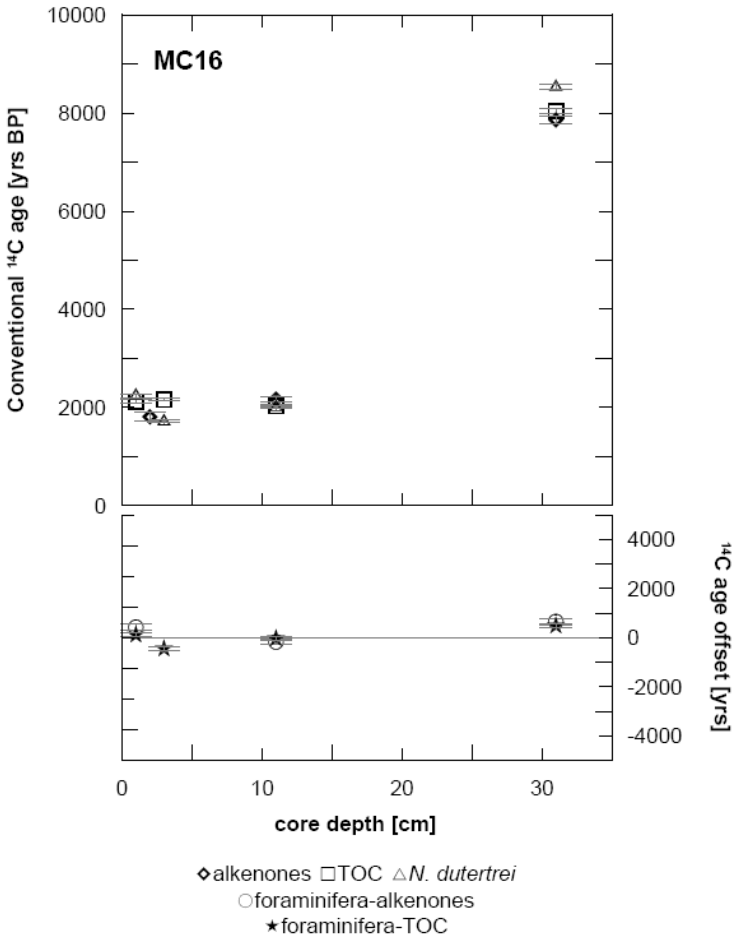


Figure 4. Conventional radiocarbon ages of alkenones, foraminifera (N. dutertrei) and Total Organic Carbon (TOC) for core MC16 and the age-offsets between alkenones and foraminifera (open circles) and TOC and foraminifera (stars). Error bars indicate 1σ analytical uncertainty (the propagated error is given in the lower panel).

Tables

| Core | Latitude (°N) | Longitude (°W) | Water depth (m) |
|---|---|---|---|
| ME0005A-24JC | 0°01.3′ | 86°27.8′ | 2941 |
| Y69-71P | 0°06′ | 86°29′ | 2740 |
| MC16 | 1°51.6′ | 86°18.3′ | 2767 |

*Table 1. Core locations.*

| | | Foraminifera | | | TOC | | Alkenones | |
|---|---|---|---|---|---|---|---|---|
| Sample | Core depth (cm) | Species | fMC | $^{14}$C age (yrs BP) | fMC | $^{14}$C age (yrs BP) | fMC | $^{14}$C age (yrs BP) |
| ME0005A-24JC | 15-20 | *N. dutertrei* | 0.6670±0.0025 | 3 255±30 | 0.6849±0.0029 | 3 040±35 | 0.6635±0.0078 | 3 290±95 |
| | 15-20 | *G. sacculifer* | 0.6794±0.0025 | 3 105±30 | | | | |
| | 46-51 | *N. dutertrei* | 0.4129±0.0022 | 7 100±40 | 0.4130±0.0024 | 7 100±45 | | |
| | 76-81 (81) | *N. dutertrei*[a] | 0.3246±0.0016 | 9 040±40 | 0.3263±0.0017 | 9 000±40 | | |
| | 226.5-231.5 (230) | *N. dutertrei*[a] | 0.1772±0.0008 | 13 900±35 | 0.1764±0.0014 | 13 950±65 | 0.1822±0.0035 | 13 650±150 |
| | 285-290 (291) | *N. dutertrei*[a] | 0.1416±0.0015 | 15 700±85 | 0.1382±0.0013 | 15 900±75 | 0.1402±0.0025 | 15 800±140 |
| | 345-351 (351) | *N. dutertrei*[a] | 0.1057±0.0009 | 18 050±65 | 0.1114±0.0010 | 17 650±75 | 0.1061±0.0021 | 18 000±160 |
| Y69-71P | 11-18 | *N. dutertrei* | 0.6681±0.0022 | 3 240±25 | 0.6530±0.0024 | 3 420±30 | 0.4120±0.0168 | 7 120±330 |
| | 11-18 | *G. sacculifer* | 0.7247±0.0023 | 2 590±25 | | | | |
| | 25-30 | *N. dutertrei* | 0.4674±0.0019 | 6 110±30 | 0.4871±0.0024 | 5 780±40 | 0.4004±0.0136 | 7 350±270 |
| | 25-30 | *G. sacculifer* | 0.4864±0.0043 | 5 790±70 | | | | |
| | 31-39 | | | | 0.4194±0.0019 | 6 980±35 | | |
| | 50 | *N. dutertrei*[b] | 0.2968±0.0015 | 9 760±40 | | | | |
| | 51-56 | *N. dutertrei* | 0.2987±0.0022 | 9 705±60 | 0.3120±0.0019 | 9 350±45 | 0.3090±0.0052 | 9 430±130 |
| | 81-89 | | | | 0.2377±0.0017 | 11 550±60 | 0.2183±0.0067 | 12 200±250 |
| | 117-123 (120) | *N. dutertrei*[b] | 0.1604±0.0013 | 14 700±65 | 0.1678±0.0017 | 14 350±80 | 0.1567±0.0047 | 14 900±240 |
| | 163-167 | | | | 0.1328±0.0014 | 16 200±80 | 0.1208±0.0036 | 17 000±240 |
| | 180 | *N. dutertrei*[b] | 0.0920±0.0008 | 19 150±70 | | | | |
| | 183-188 | *N. dutertrei* | 0.1106±0.0019 | 17 690±140 | 0.0979±0.0013 | 18 650±110 | 0.0998±0.0024 | 18 500±200 |
| | 253-258 | *N. dutertrei* | 0.0350±0.0016 | 26 920±370 | 0.0521±0.0009 | 23 700±130 | 0.0531±0.0015 | 23 600±230 |
| | 260 | *N. dutertrei*[a] | 0.0305±0.0007 | 28 000±190 | | | | |
| MC16 | 0-4 | | | | | | 0.7981±0.0085 | 1 810±85 |
| | 1-2 | *N. dutertrei* | 0.7565±0.0034 | 2 240±35 | 0.7682±0.0033 | 2 120±35 | | |
| | 3-4 | *N. dutertrei* | 0.8076±0.0030 | 1 715±30 | 0.7644±0.0027 | 2 160±30 | | |
| | 11-12 | *N. dutertrei* | 0.7792±0.0029 | 2 005±30 | 0.7768±0.0030 | 2 030±30 | 0.7630±0.0059 | 2 170±60 |
| | 31-32 | *N. dutertrei* | 0.3458±0.0022 | 8 530±50 | 0.3675±0.0021 | 8 040±45 | 0.3760±0.0039 | 7 860±80 |

Table 2. Radiocarbon data (fMC; fraction modern carbon and conventional $^{14}$C ages) of foraminifera, TOC and alkenones of cores ME0005A-24JC, Y69-71P and MC16. Depths in parentheses refer to foraminiferal samples, if different from organic matter samples. Analytical uncertainties are given as 1σ-analytical errors. (a) data from Kienast et al. (2007), (b) data from Clark et al. (2004).

**Appendix: Supplementary data**

A. Potential effects of sediment transport on $U_{37}^{k'}$ derived sea surface temperatures

Comparison of the $U_{37}^{k'}$ derived SSTs of both cores ME0005-24JC and Y69-71P published by *Kienast et al.* (2006) and *Prahl et al.* (2006) shows a general temperature offset of approximately 1 to 1.5°C (with Y69-71P being colder) although both cores should reflect the same SST due to their proximity. If we use our $^{14}C$ data to develop a new age model for core Y69-71P, the temperature offset is reduced for the deglacial and disappears for the early to middle Holocene. But for the uppermost core depths, reflecting the late Holocene, the temperature offset of ~1°C remains. This offset prevails mainly in the core interval where our data show alkenones older than foraminifera and TOC (11-18cm and 25-30cm).

We can calculate the potential contribution of alkenones reflecting colder temperatures (e.g. the time interval of Heinrich event 1 (H1)) and use isotopic mass balance to quantify the likely effect on the $^{14}C$ age assuming that the $U_{37}^{k'}$ derived SSTs estimated for core ME0005-24JC reflect the "true" SSTs. For depth interval 25-30cm an H1 alkenone contribution of approximately 17% (fMC=0.1567) alters the "true" alkenone depositional age (fMC=0.4674; assumed to be reflected by the equivalent foraminiferal age) to the actually measured age (fMC=0.4004 measured; fMC=0.4140 calculated). Therefore, if the observed age offset between alkenones and foraminifera and TOC for depth intervals 25-30cm is real, contribution of older alkenones (H1) could be a potential explanation for that age offset. Contrary, the age offset evident for depth interval 11-18cm cannot be explained by contribution of approximately 22% of H1 alkenones alone. Applying the same mass balance equation as above does not alter the alkenone age sufficiently (fMC=0.4120 measured; fMC=0.5556 calculated).

If, as discussed above, the alkenone contamination is radiocarbon dead (fMC=0) we can quantify the $U_{37}^{k'}$ derived SST signal of those advected alkenones. The mass balance derived potential contamination of 38% for depth interval 11-18cm (5.1.1) would require alkenones synthesized in sea surface waters with approximately 22.7°C. This temperature is well within the range of the temperatures for the time interval 50-150kyr measured by *Prahl et al.* [2006]. Again, if the observed age offset between alkenone and foraminiferal and TOC $^{14}C$ ages is real, addition of $^{14}C$-free alkenones might be a possible explanation. As discussed above, the material is likely to be delivered from nearby topography. However, the potential source areas (surrounding abyssal hills) must have been different at the respective times to explain the different ages (H1 vs. >50kyr) required for the advected alkenones to result in the measured age offsets to foraminifera and TOC.

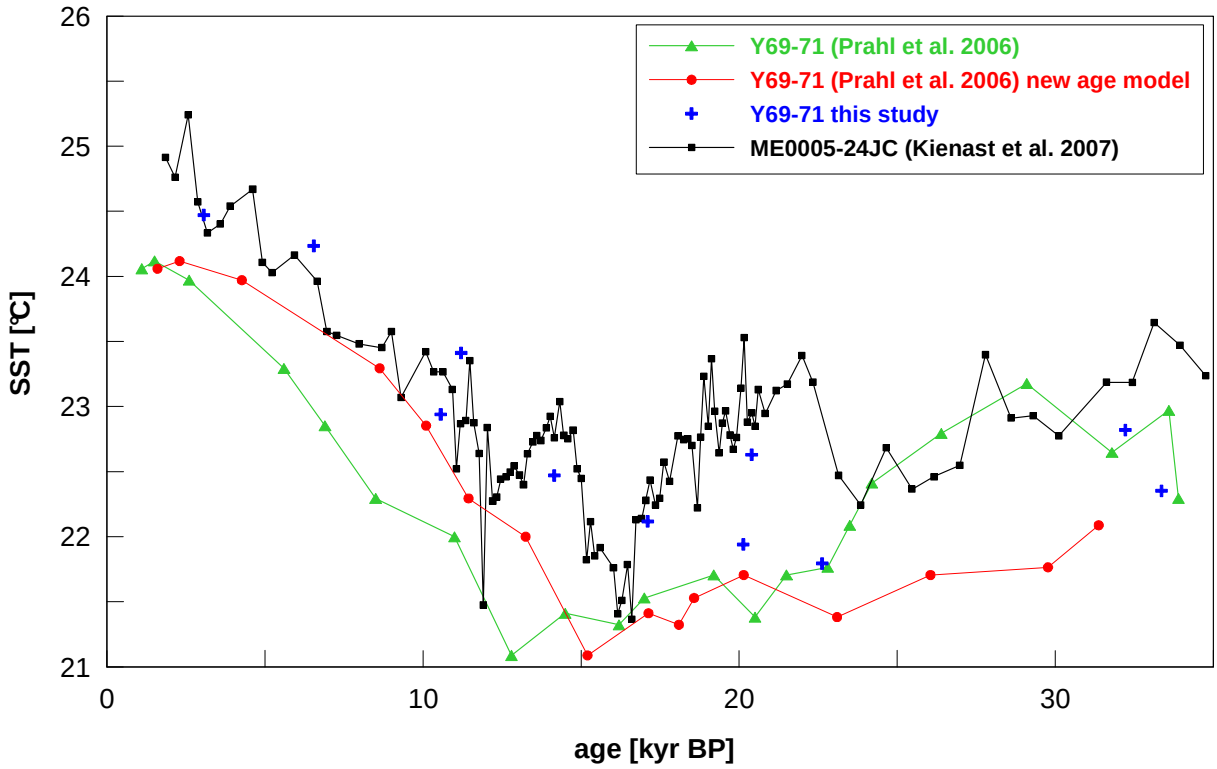


*Figure 5. $U^{k'}_{37}$ derived SSTs for core ME0005-24JC (Kienast et al. 2007) and Y69-71P (Prahl et al. 2006; this study). For core Y69-71P SSTs are additionally plotted using a modified age model based on our foraminiferal $^{14}C$ results.*

B. Receipt numbers of radiocarbon analysis

| Sample | | Foraminifera | | TOC | Alkenones |
|---|---|---|---|---|---|
| | Core depth (cm) | Species | receipt # | receipt # | receipt # |
| ME0005A-24JC | 15-20 | *N. dutertrei* | *KIA 34472* | 58954 | 58950 |
| | 15-20 | *G. sacculifer* | *KIA 34471* | | |
| | 46-51 | *N. dutertrei* | 66556 | 66554 | |
| | 76-81 | | | 66555 | |
| | 81 | *N. dutertrei* | 33431 | | |
| | 226,5-231,5 | | | 58955 | 58951 |
| | 230 | *N. dutertrei* | 33432 | | |
| | 285,5-290,5 | | | 58956 | 58952 |
| | 291 | *N. dutertrei* | 33433 | | |
| | 345-350 | | | 58957 | 58953 |
| | 351 | *N. dutertrei* | 33434 | | |
| Y69-71P | 11-18 | *N. dutertrei* | 43983 | 43167 | 43161 |
| | 11-18 | *G. sacculifer* | 43984 | | |
| | 25-30 | *N. dutertrei* | 43985 | 43168 | 43162 |
| | 25-30 | *G. sacculifer* | 43986 | | |
| | 31-39 | | | 40605 | |
| | 51-56 | *N. dutertrei* | *KIA 35966* | 63256 | 63250 |
| | 81-89 | | | 40607 | 40722 |
| | 117-123 | | | 40608 | 40723 |
| | 120 | *N. dutertrei* | 33428 | | |
| | 163-167 | | | | |
| | 183-188 | *N. dutertrei* | *KIA 35967* | 63257 | 63251 |
| | 253-258 | *N. dutertrei* | *KIA 35968* | 63258 | 63252 |
| MC16 | 1-2 | *N. dutertrei* | *KIA 35969* | 63259 | |
| | 3-4 | *N. dutertrei* | *KIA 35970* | 63260 | |
| | 0-4 | | | | 63253 |
| | 10-12 | | | | 63254 |
| | 11-12 | *N. dutertrei* | *KIA 35971* | 63261 | |
| | 30-32 | | | | 63255 |
| | 31-32 | *N. dutertrei* | *KIA 35972* | 63262 | |

*Table 3. Receipt numbers from NOSAMS and Leibniz laboratory (KIA numbers, in italics).*